

# Arginyl-fructosyl-glucose from red ginseng alleviates TGF- $\beta$ 1-induced epithelial-mesenchymal transition of renal tubular epithelial cells

Xiangdong Lin<sup>1,\*</sup>, Ming Xiang<sup>2,\*</sup>, Haiying Chen<sup>3</sup> and Xinyu Chen<sup>4</sup>

<sup>1</sup> Department of Endocrinology, The First Hospital of Hunan University of Chinese Medicine, Changsha, Hunan, P.R. China

<sup>2</sup> Department of Diagnostics of Traditional Chinese Medicine, Hunan University of Chinese Medicine, Changsha, Hunan, P.R. China

<sup>3</sup> Department of Nephrology, The First Hospital of Hunan University of Chinese Medicine, Changsha, Hunan, P.R. China

<sup>4</sup> The First Hospital of Hunan University of Chinese Medicine, Changsha, Hunan, P.R. China

**Abstract.** This study aims to explore the effect and mechanism of arginyl-fructosyl-glucose (AFG) on TGF- $\beta$ 1-induced epithelial-mesenchymal transition (EMT) of renal tubular epithelial cells. HK-2 cells were induced by TGF- $\beta$ 1 and then co-cultured with AFG at different concentrations (0, 25, 50, and 100  $\mu$ mol/l) for 48 h. The morphology of HK-2 cells was observed under an inverted microscope and the expressions of  $\alpha$ -SMA, Vimentin, and E-cadherin were assessed by qRT-PCR, Western blot, and immunofluorescence. The mRNA expressions of ERK and STAT3 were also examined by qRT-PCR, and the protein levels of ERK, STAT3, p-ERK, and p-STAT3 were measured by Western blot. Finally, CCK-8 and transwell assays were used to detect cell proliferation and invasion. TGF- $\beta$ 1 treatment significantly induced EMT in HK-2 cells. The expressions of p-ERK and p-STAT3 were significantly increased after TGF- $\beta$ 1 induction, while Mogrol treatment inhibited p-ERK, p-STAT3,  $\alpha$ -SMA, and Vimentin expression levels, enhanced E-cadherin expression, and suppressed cell proliferation and invasion. AFG exposure could also inhibit p-ERK, p-STAT3,  $\alpha$ -SMA, and Vimentin expressions, promote E-cadherin expression, and markedly inhibit HK-2 cell proliferation and invasion. AFG inhibited TGF- $\beta$ 1-induced EMT of renal tubular epithelial cells by regulating phosphorylation of ERK and STAT3.

**Key words:** Arginyl-fructosyl-glucose — Renal tubular epithelial cell — TGF- $\beta$ 1 — ERK — STAT3 — Epithelial-mesenchymal transition

## Introduction

Chronic kidney disease (CKD) is an important public-health issue, with an estimated incidence of 8–16% worldwide (Jha et al. 2013). Kidney fibrosis is an inevitable pathophysiologic change in CKD progression (Gupta et al. 2020). Epithelial-

mesenchymal transition (EMT) is one of the most important causes of renal interstitial fibrosis (RIF), and in RIF progression, the EMT process is characterized by the acquisition of mesenchymal phenotype and myofibroblast functions by renal tubular epithelial cells (Ghosh et al. 2021). Growing number of evidences supports that EMT process is a crucial event for dealing with fibrotic disorders in CKD (Kang 2018; Hu et al. 2021).

Extracellular signal-regulated kinases (ERK) are one of the classic transduction pathways of mitogen-activated protein kinases (MAPK) family. At present, many studies have shown that ERK signaling pathway was closely related to renal fibrosis. For example, fraxetin inhibited the progres-

\* These authors contributed equally to the research.

**Correspondence to:** Xinyu Chen, The First Hospital of Hunan University of Chinese Medicine, No.95 Shaoshan Mid Rd, Yuhua District, Changsha, Hunan 410007, P.R. China  
E-mail: chenxinyu1962@163.com

sion of renal fibrosis by regulating ERK signaling (Hsieh et al. 2021). Mulberry leaves inhibited RIF by activating ERK signaling (Ji et al. 2019). STAT3 is an important regulatory element downstream of ERK cascade, and ERK specifically phosphorylates tryptophan 727 on STAT3 to regulate and enhance the transcriptional activity of STAT3. STAT3 inhibitor S3I-201 could improve renal dysfunction, reduce serum uric acid level, and delay the progression of renal fibrosis (Pan et al. 2021). However, the relationship between ERK/STAT3 pathway and EMT-induced RIF has not been deeply studied.

Red ginseng (*Panax ginseng* Meyer) shows high efficiency of inhibiting inflammation, anti-fibrotic activity, and other pharmacological effects in renal disease (Karunasagara et al. 2020), mainly caused by ginsenosides in red ginseng (Park et al. 2017; Wang et al. 2021). Ginsenosides extracted from red ginseng could act an anti-proliferative effect by inhibiting the phosphorylation of ERK (Lee et al. 2017). Red ginseng and its ginsenosides could effectively alleviate chemotherapy-induced toxicity on kidney, liver, heart, and immune and hematopoietic inhibition, which might involve with ERK signaling pathway (Wan et al. 2021). During the processing of red ginseng, some non-saponins active substances are still produced. Arginyl-fructosyl-glucose (AFG) is an important non-saponin active substance that belongs to arginine derivatives, and shows substantial antioxidant activity and anti-inflammatory effect (Liu et al. 2020). At the same time, AFG has a strong protective effect on kidney injury (Li et al. 2019). However, there are fewer studies on the exact role and mechanisms of this non-saponin in renal fibrosis.

A large number of studies have shown that TGF- $\beta$ 1 can induce renal tubular EMT and lead to renal fibrogenesis (Zhang et al. 2017; Ma et al. 2018). This study aims to investigate whether AFG could regulate the activation of ERK/STAT3 signaling pathway to intervene the EMT of renal tubular epithelial cells. To this end, TGF- $\beta$ 1 is utilized to mimic renal fibrosis *in vitro*, and then the effects of AFG on experimentally-induced EMT in renal epithelial cells and ERK/STAT3 signaling pathway activation are evaluated, which may propose a novel therapeutic agent for the treatment of RIF.

## Materials and Methods

### Cell culture

Human renal tubular epithelial cells (HK-2) were purchased from American Type Culture Collection (Manassas, VA, USA). Cells were maintained with DMEM/F12 medium (Gibco, Grand Island, NY, USA) containing 10% fetal bovine serum (FBS), penicillin (100 U/ml), and streptomycin (100  $\mu$ g/ml). Culture conditions were set at 37°C and 5% CO<sub>2</sub>.

### Preparation of AFG

Red ginseng is evaporated from fresh ginseng by Maillard reaction, and during this processing, AFG is produced due to the reaction of arginine and maltose. By referring to the method of Li et al. (2019), AFG was prepared by reacting arginine and maltose under anhydrous acidic conditions at 80°C for 120 min. The purity of AFG was more than 90% as measured by high performance liquid chromatography (HPLC).

### Cell induction and treatment

When the cells were at 80% confluence, the experiment was performed and TGF- $\beta$ 1 induction was based on the method of Zhang et al. (2017). Mogrol is an inhibitor of ERK and STAT3. HK-2 cells were cultured in serum-free DMEM/F12 medium and starved for 12 h, and then grouped according to different treatment methods as follows:

- (1) Control group: cells were cultured in serum-free DMEM/F12 medium for 48 h.
- (2) TGF- $\beta$ 1 group: cells were cultured in serum-free DMEM/F12 medium containing aqua sterilisata-dissolved TGF- $\beta$ 1 (5 ng/ml, Abcam, Cambridge, UK) for 48 h.
- (3) TGF- $\beta$ 1+NaCl group: cells were cultured in serum-free DMEM/F12 medium containing TGF- $\beta$ 1 (5 ng/ml) and 0.9% NaCl solution for 48 h.
- (4) TGF- $\beta$ 1+25AFG group: cells were cultured in serum-free DMEM/F12 medium containing TGF- $\beta$ 1 (5 ng/ml) and AFG liquor (25  $\mu$ mol/l, dissolved in 0.9% NaCl solution) for 48 h.
- (5) TGF- $\beta$ 1+50AFG group: cells were cultured in serum-free DMEM/F12 medium containing TGF- $\beta$ 1 (5 ng/ml) and AFG (50  $\mu$ mol/l, dissolved in 0.9% NaCl solution) for 48 h.
- (6) TGF- $\beta$ 1+100AFG group: cells were cultured in serum-free DMEM/F12 medium containing TGF- $\beta$ 1 (5 ng/ml) and AFG (100  $\mu$ mol/l, dissolved in 0.9% NaCl solution) for 48 h.
- (7) TGF- $\beta$ 1+DMSO group: cells were cultured in serum-free DMEM/F12 medium containing TGF- $\beta$ 1 (5 ng/ml) and an equal volume of dimethyl sulfoxide (DMSO, Abcam, Cambridge, MA, USA) for 48 h.
- (8) TGF- $\beta$ 1+Mogrol group: cells were cultured in serum-free DMEM/F12 medium containing TGF- $\beta$ 1 (5 ng/ml) and Mogrol (250  $\mu$ mol/l, dissolved in DMSO, Bangjing, Shanghai, China) for 48 h.

### Cell morphology

Cells in each group were observed under a microscope (Olympus CKX41, Olympus Co., Ltd., Tokyo, Japan) before or after treatment with TGF- $\beta$ 1 to monitor cell morphology and verify the effect of AFG on HK-2 cells.

*Real time qPCR (qRT-PCR)*

Total RNA was extracted using Trizol (15596026, Invitrogen, Car, USA) and reverse transcribed into cDNA using reverse transcription kit (RR047A, Takara, Japan), with a reaction system of 20  $\mu$ l. The reaction condition was as follows: reaction at 37°C for 15 min and at 85°C for 5 s. The RNA samples were loaded using SYBR Premix EX Taq Kit (RR420A, Takara). The samples were subjected to real time fluorescence quantitative PCR (ABI7500, ABI, Foster City, CA, USA). The reaction system consisted of 9  $\mu$ l SYBR Mix, 0.5  $\mu$ l forward primer, 0.5  $\mu$ l reverse primer, and 8  $\mu$ l RNase Free dH<sub>2</sub>O. The reaction conditions were: predenaturation at 95°C for 10 min, denaturation at 95°C for 15 s, annealing at 60°C for 1 min, in a total of 40 cycles. The Ct values of each well were recorded, with GAPDH as the internal reference. Relative expression of genes was calculated using  $2^{-\Delta\Delta Ct}$  method.  $\Delta\Delta Ct = [Ct(\text{target gene}) - Ct(\text{housekeeping gene})]_{\text{experimental group}} - [Ct(\text{target gene}) - Ct(\text{housekeeping gene})]_{\text{control group}}$ . Each experiment was repeated three times independently, and three replicate wells were set for each sample. Related primers were designed by Shanghai Sangon Biotech. Primer sequences are detailed in Table 1.

*Western blot*

After cells were lysed with RIPA lysis buffer (Beyotime), BCA detection kit (Beyotime) was used to detect the protein concentration. The loading buffer was added and mixed with the protein before a 3-min boiling water bath. After that, electrophoresis was performed at 80 V for 30 min, and then at 120 V for 1–2 h instead after bromophenol blue entered the separation gel. The membrane transferring was performed in an ice bath with a current of 300 mA for 60 min, and then the membrane was rinsed with for 1–2 min and sealed for 60 min at room temperature or blocked at 4°C overnight. The membrane was incubated with primary antibodies against GAPDH (ab9485, 1:2500, Abcam),  $\alpha$ -SMA (ab124964, 1:10000, Abcam), Vimentin (ab92547, 1:1000, Abcam), E-cadherin (ab40772, 1:10000, Abcam), ERK (ab184699, 1:10000, Abcam), p-ERK (ab229912, 1:1000, Abcam), STAT3 (ab68153, 1:1000, Abcam), and p-STAT3 (Cell Signaling Technology, Massachusetts, USA) on a shaker at room temperature for 1 h, and washed for 3 times, 10 min each time. Then secondary antibody (goat anti-rabbit IgG labeled with horseradish peroxidase, 1:5000, Beijing ComWin Biotech Co., Ltd., Beijing, China) was added for a 1-h incubation at room temperature, followed by washing for three times, 10 min each time. Finally, chemiluminescence imaging system (Bio-Rad) was used for detection after color development. Each experiment was repeated three times independently and three replicate wells were set for each sample.

*CCK-8 assay*

The transfected cells in each group were inoculated onto a 96-well plate with 100  $\mu$ l diluted cell suspension ( $1 \times 10^5$  cells/ml) *per* well. After the cells were incubated in the incubator for respectively 0, 24, 48, 72, and 96 h, 10  $\mu$ l of CCK-8 reagent (Tokyo, Dojindo, Japan) was added into each well for a 2-h incubation. The absorbance was measured at a wavelength of 450 nm. Each experiment was repeated three times independently and three replicate wells were set for each sample.

*Transwell assay*

For Matrigel activation, the chamber covered with Matrigel was taken out from a -20°C refrigerator and melted at room temperature, and serum-free medium (0.5 ml) was added to transwell chamber (Corning, New York, USA) and 24-well plate for a 2-h incubation under a condition of 37°C and 5% CO<sub>2</sub>, followed by removal of culture medium. Cells in logarithmic growth phase were collected, prepared into single cell suspension, and uniformly inoculated in a 6-well plate. Cells were cultured in a 5% CO<sub>2</sub> incubator at 37°C. When the cell confluence reached 70–90%, the cells in each group were treated as above stated. Then the cells were cultured in a 5% CO<sub>2</sub> incubator at 37°C for 24 h. After that, the cells were digested with trypsin, washed twice with PBS, and resuspended in serum-free DMEM medium to adjust cell concentration. Medium (600  $\mu$ l) containing 10% FBS was added to the basolateral chamber, and cell suspension (100  $\mu$ l) was added to the apical chamber, followed by cell culture for 24 h at 37°C and 5% CO<sub>2</sub>. Then the apical chamber was taken out, with supernatant discarded. The non-invaded cells on the upper surface were removed with cotton swabs and invaded cells on the lower surface

**Table 1.** Primer sequences used in qRT-PCR analysis

Primer	Sequences
$\alpha$ -SMA-F	CTATGAGGGCTATGCCTTGCC
$\alpha$ -SMA-R	GCTCAGCAGTAGTAACGAAGGA
Vimentin-F	TGACCGCTTCGCCAACTACAT
Vimentin-R	TCCCGCATCTCCTCCTCGTA
E-cadherin-F	ATTTTTCCCTCGACACCCGAT
E-cadherin-R	TCCAGGCGTAGACCAAGA
ERK-F	CAGTTCTTGACCCCTGGTCC
ERK-R	TACATACTGCCGACAGGTCAC
STAT3-F	AGCAGCACCTTCAGGATGTC
STAT3-R	GCATCTTCTGCCTGGTCACT
GAPDH-F	AATGGGCAGCCGTTAGGAAA
GAPDH-R	GCGCCAATACGACCAAATC

F, forward; R, reverse.

were fixed with 4% paraformaldehyde for 20 min. After Wright-Giemsa staining, the cells were photographed using a microscope in five randomly selected fields. Each experiment was repeated three times independently.

#### Immunofluorescence (IF)

Cells were fixed with paraformaldehyde (4%) in PBS (0.1 mol/l), and then sealed with normal goat serum (10%) for 1 h. The fixed cells were incubated with primary antibodies against  $\alpha$ -SMA (ab124964, 1:250), Vimentin (ab92547, 1:250), and E-cadherin (ab40772, 1:500, Abcam) at 4°C overnight. Subsequently, the secondary antibody IgG was added for incubation for 1 h after the cells were washed

with PBS. Finally, the cells were stained with 4',6-diamidino-2-phenylindole (DAPI) and treated with Vectashield Mounting Media (Vector Laboratories Inc., Burlingame, CA). Images were recorded with a fluorescence microscope (Leica, TCSSP2, German) at 400 times magnification. Each experiment was repeated three times independently, with five fields of vision observed.

#### Statistical analysis

Data were analyzed by GraphPad prism7 software, and expressed as mean  $\pm$  standard deviation ( $\pm$  SD). T-test and one-way analysis of variance were used for comparisons between two groups and among groups, respectively. Tukey's

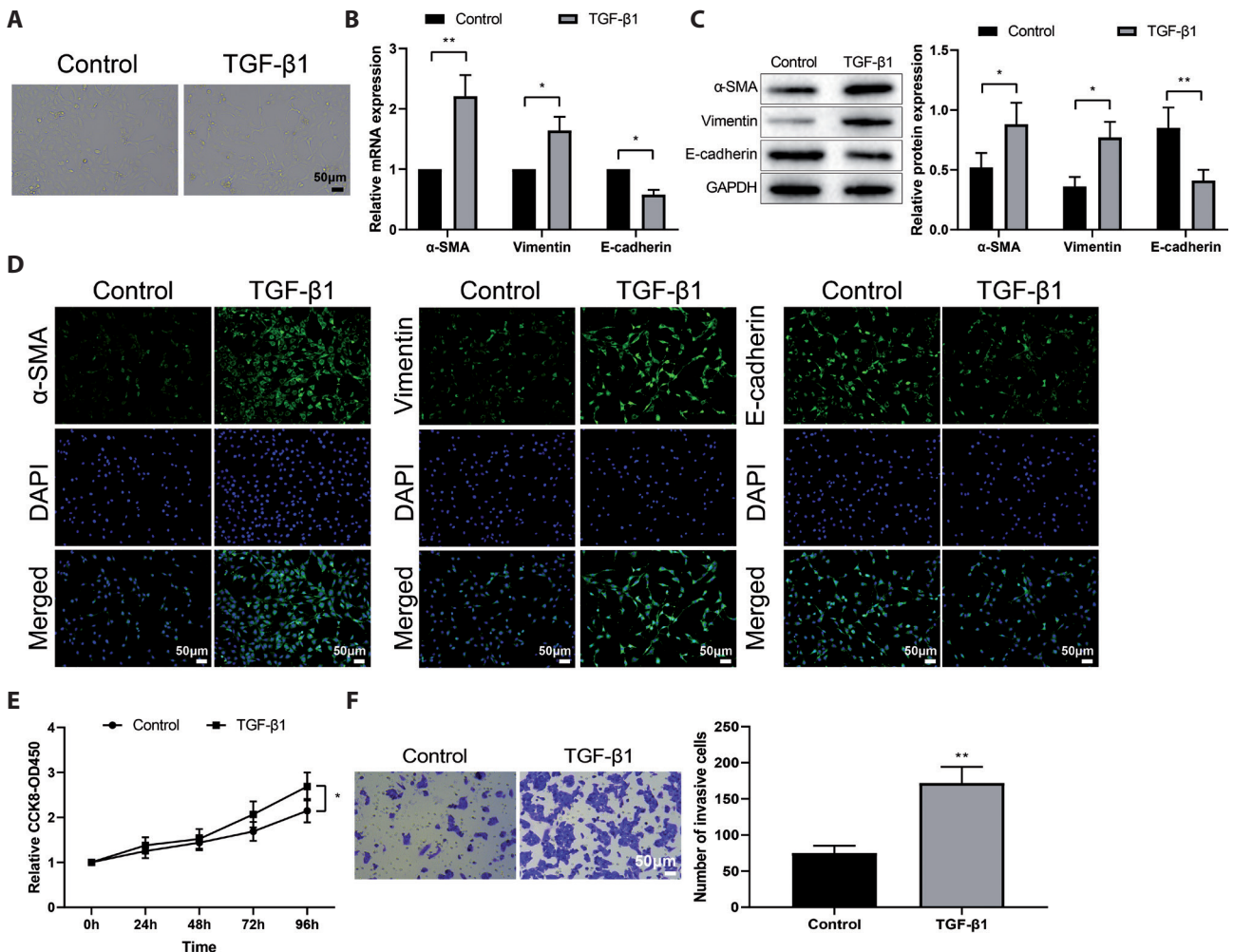


**Figure 1.** TGF- $\beta$ 1 could induce epithelial-mesenchymal transition in HK-2 cells. **A.** Morphological changes of HK-2 cells observed under microscope. The expressions of  $\alpha$ -SMA, Vimentin, and E-cadherin were evaluated by qRT-PCR (**B**), Western blot (**C**), and immunofluorescence (**D**). Cell proliferation and invasion were measured by CCK-8 (**E**) and transwell (**F**) assays. \*  $p < 0.05$ , \*\*  $p < 0.01$  compared with Control group. The measurement data were expressed as mean  $\pm$  SD ( $n = 15$  for immunofluorescence and transwell assays;  $n = 9$  for other experiments). Comparisons between two groups were performed using t-test. The scale = 50  $\mu$ m.

multiple comparisons test was used for *post hoc* analysis.  $p < 0.05$  was considered significant. All experiments were repeated three times.

## Results

### *TGF- $\beta$ 1 induced EMT in HK-2 cells*

To investigate the effect of AFG on TGF- $\beta$ 1-induced renal tubular cell EMT, we used TGF- $\beta$ 1 to induce EMT in HK-2 cells. The microscopic observation result showed that normal HK-2 cells were oval and closely connected in Control group, while cells were signally longer and loosely spread in TGF- $\beta$ 1 group (Fig. 1A). The expressions of  $\alpha$ -SMA, Vimentin, and E-cadherin were measured by qRT-PCR and Western blot. The results showed that in TGF- $\beta$ 1 group, the expressions of  $\alpha$ -SMA and Vimentin were markedly increased but E-cadherin expression was markedly decreased (*vs.* Control group) (Fig. 1B and C).

The results of IF revealed that E-cadherin on cell membrane was continuously linear distributed, and  $\alpha$ -SMA and Vimentin seldom expressed in Control group. After TGF- $\beta$ 1 induction, E-cadherin on cell membrane was distributed in moth-eaten shape and the expressions of  $\alpha$ -SMA and Vimentin were signally enhanced (Fig. 1D). CCK-8 and transwell results showed that cell proliferation and invasion abilities were significantly strengthened in TGF- $\beta$ 1 group compared with TGF- $\beta$ 1 group (Fig. 1E and F). These results have provided evidence that TGF- $\beta$ 1 could induce EMT in HK-2 cells.

### *TGF- $\beta$ 1 induced EMT via ERK/STAT3 signaling pathway*

To verify the implication of ERK/STAT3 signaling pathway in TGF- $\beta$ 1-induced EMT in HK-2 cells, the mRNA levels of ERK and STAT3 were firstly detected by qRT-PCR. Result revealed that the levels of ERK and STAT3 mRNAs showed no marked differences in TGF- $\beta$ 1 group (*vs.* Control group) and TGF- $\beta$ 1+Mogrol group (*vs.* TGF- $\beta$ 1+DMSO group) (Fig. 2A). The protein levels of ERK, STAT3, p-ERK and p-STAT3 in HK-2 cells were measured by Western blot. The results showed that the protein levels of p-ERK and p-STAT3 were observably increased in TGF- $\beta$ 1 group compared with Control group, while those in TGF- $\beta$ 1+Mogrol group were inhibited compared with TGF- $\beta$ 1+DMSO group. There was no significant difference in the expressions of ERK and STAT3 among the groups (Fig. 2B).

Next, the expressions of  $\alpha$ -SMA, Vimentin, and E-cadherin were measured by qRT-PCR and Western blot. The results showed that the expressions of  $\alpha$ -SMA and Vimentin were significantly decreased, while E-cadherin expression was significantly increased in TGF- $\beta$ 1+Mogrol group (*vs.*

TGF- $\beta$ 1+DMSO group) (Fig. 2C and D). Additionally, IF results revealed a marked increase of E-cadherin and obvious decreases of  $\alpha$ -SMA and Vimentin in TGF- $\beta$ 1+Mogrol group (*vs.* TGF- $\beta$ 1+DMSO group) (Fig. 2E). CCK-8 and transwell results showed that cell proliferation and invasion abilities were reduced in TGF- $\beta$ 1+Mogrol group compared with TGF- $\beta$ 1+DMSO group (Fig. 2F and G). Above results indicated that phosphorylation of ERK and STAT3 was an important form of its involvement in related biological activities, while the change of total protein was relatively constant. TGF- $\beta$ 1 could promote EMT of HK-2 cells through phosphorylation of ERK and STAT3.

### *AFG inhibited phosphorylation of ERK and STAT3*

The chemical structural formula of AFG is shown in Figure 3A. In our study, the EMT of HK-2 cells were induced by 5 ng/ml TGF- $\beta$ 1, during which the cells were co-cultured with different concentrations of AFG (0, 25, 50, and 100  $\mu$ mol/l) for 48 h.

First, the mRNA levels of ERK and STAT3 were measured by qRT-PCR. There was no obvious difference among the four groups (Fig. 3B), which suggested that AFG intervention could not affect the mRNA levels of ERK and STAT3. Subsequently, the protein levels of ERK, STAT3, p-ERK, and p-STAT3 were measured by Western blot. The results showed signally increases of the levels of p-ERK and p-STAT3 and insignificant changes in ERK and STAT3 levels in TGF- $\beta$ 1+100AFG group (*vs.* TGF- $\beta$ 1+NaCl group) (Fig. 3C). Above results indicated that AFG intervention could partially inhibit phosphorylation of ERK and STAT3.

### *AFG could inhibit TGF- $\beta$ 1-induced EMT*

After HK-2 cells were induced EMT by 5 ng/ml. TGF- $\beta$ 1 and co-cultured with different concentrations of AFG (0, 25, 50, 100  $\mu$ mol/l), the morphologic changes of the cells were observed under an inverted microscope. The results showed that cells were spindle-shaped in TGF- $\beta$ 1+NaCl group (Fig. 4A). In TGF- $\beta$ 1+100AFG group, the morphology of cells were markedly improved. Specifically, most of them were oval and adhered to the wall, and the number of floating cells were signally decreased (Fig. 4A).

The expressions of  $\alpha$ -SMA, Vimentin, and E-cadherin were measured by qRT-PCR and Western blot. When compared with TGF- $\beta$ 1+NaCl group, TGF- $\beta$ 1+100AFG group showed decreased expressions of  $\alpha$ -SMA and Vimentin but increased E-cadherin expression. While there was no marked statistical difference in the expressions of  $\alpha$ -SMA, Vimentin, and E-cadherin in TGF- $\beta$ 1+25AFG group and TGF- $\beta$ 1+50AFG group, relative to TGF- $\beta$ 1+NaCl group (Fig. 4B and C). IF results revealed that E-cadherin expression was signally increased, while the expressions of  $\alpha$ -SMA

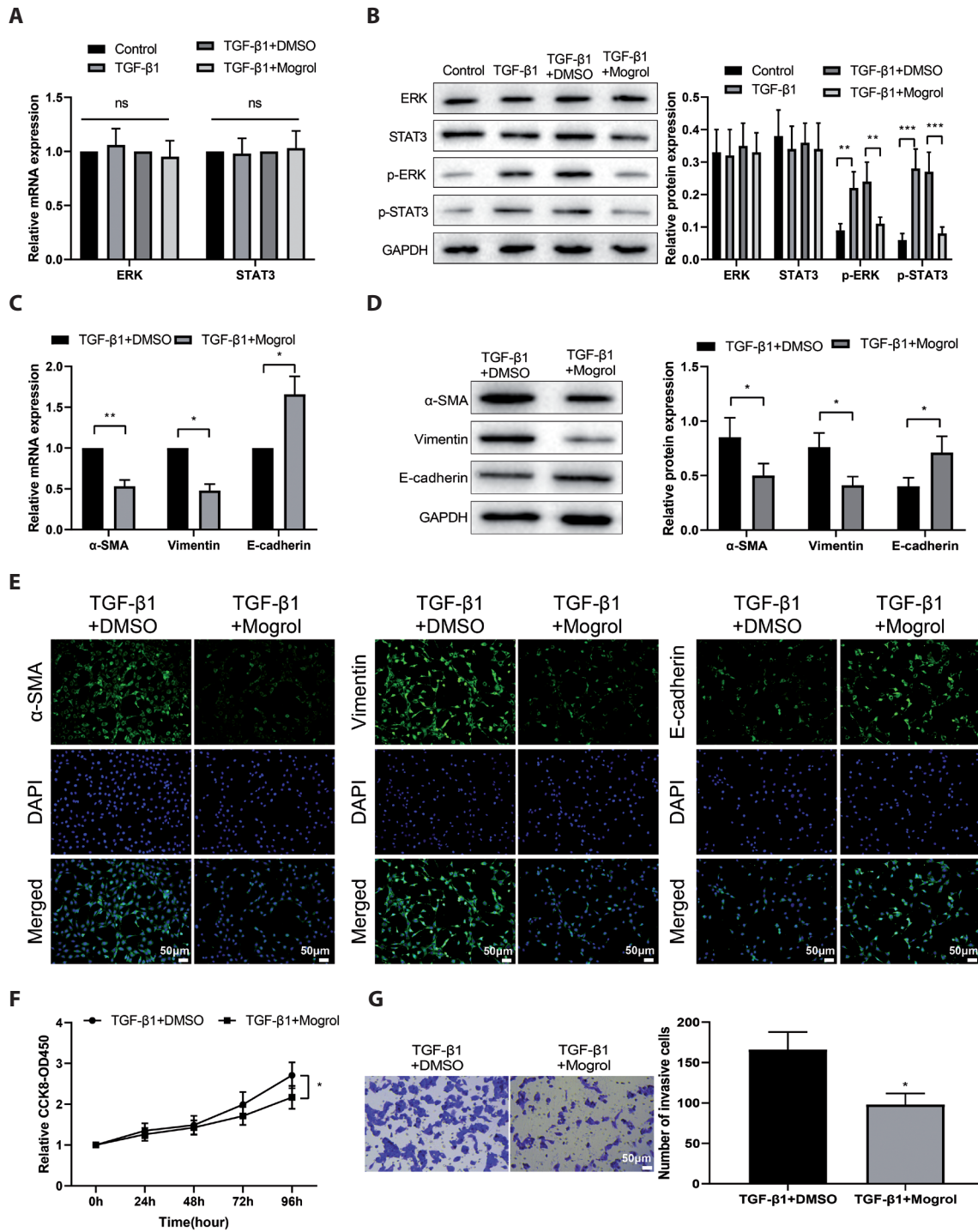


**Figure 2.** TGF-β1 could induce HK-2 cell epithelial-mesenchymal transition by ERK/STAT3 signaling pathway. **A.** The mRNA levels of ERK and STAT3 examined by qRT-PCR. **B.** The protein levels of ERK, STAT3, p-ERK, and p-STAT3 assessed by Western blot. The expressions of α-SMA, Vimentin, and E-cadherin were evaluated by qRT-PCR (C), Western blot (D) and immunofluorescence (E). Cell proliferation and invasion were measured by CCK-8 (F) and transwell (G) tests. \*  $p < 0.05$ , \*\*  $p < 0.01$ , \*\*\*  $p < 0.001$  compared with Control group or TGF-β1+DMSO group. The measurement data were expressed as mean ± SD ( $n = 15$  for immunofluorescence and transwell experiments;  $n = 9$  for other experiments). Comparisons between two groups were performed using t-test and differences among multiple groups were assessed using one-way analysis of variance. The scale = 50 μm. ns, non significant.

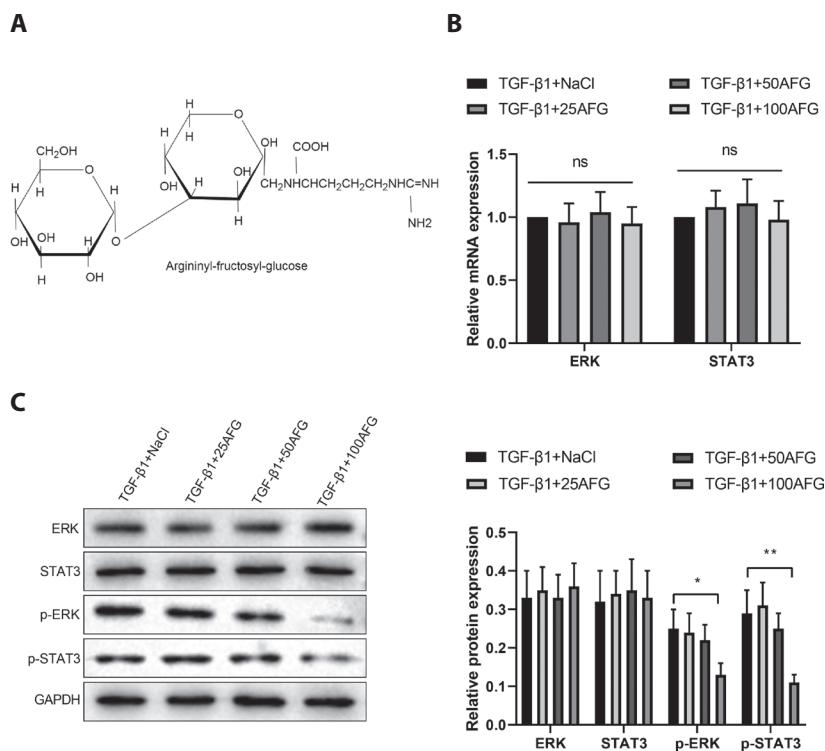


**Figure 3.** Arginyl-fructosyl-glucose inhibited the phosphorylation of ERK and STAT3 in HK-2 cells. **A.** The chemical structural formula of arginyl-fructosyl-glucose. **B.** The mRNA levels of ERK and STAT3 examined by qRT-PCR. **C.** The protein levels of ERK, STAT3, p-ERK, and p-STAT3 measured by Western blot. \*  $p < 0.05$ , \*\*  $p < 0.01$ , compared with TGF- $\beta$ 1+NaCl group. The measurement data were expressed as mean  $\pm$  SD. Differences among multiple groups were assessed using one-way analysis of variance ( $n = 9$ ). ns, non significant.

and Vimentin were signally decreased in TGF- $\beta$ 1+100AFG group (vs. TGF- $\beta$ 1+NaCl group) (Fig. 4D). CCK-8 and transwell results showed that cell proliferation and invasion abilities were obviously reduced in TGF- $\beta$ 1+100AFG group compared with TGF- $\beta$ 1+NaCl group (Fig. 4E and F,  $p < 0.05$ ). Above results suggested that AFG could reverse TGF- $\beta$ 1-induced EMT in HK-2 cells.

## Discussion

In the current study, we studied the function of AFG as an anti-fibrotic modulator in the development of TGF- $\beta$ 1-induced EMT in renal tubular epithelial cells through the ERK/STAT3 signaling pathway. Firstly, functional experiments proved that TGF- $\beta$ 1 could activate ERK/STAT3 signaling pathway to promote EMT in renal tubular epithelial cells, AFG could inhibit the phosphorylation of ERK and STAT3. Moreover, our findings suggested that AFG could alleviate TGF- $\beta$ 1-induced EMT in renal tubular epithelial cells. Our results may offer novel insights into the treatment and prevention of RIF.

Transforming growth factor- $\beta$  (TGF- $\beta$ ), the prototype of the TGF- $\beta$  family of growth and differentiation factors, is a potent fibrogenic cytokine implicated in pathological changes in various organs including the kidney (Morikawa et al. 2016). Although EMT can be stimulated by several

inducers (Ghosh et al. 2021), a plenty of works have identified that TGF- $\beta$ 1 is sufficient to induce EMT in experimental models of CKD (Yu et al. 2019; Wang et al. 2020). It has been reported as the principal driver of tissue scarring leading to interstitial renal fibrosis and affected p53 phosphorylation in renal fibrogenesis (Higgins et al. 2018). In our study, we firstly used TGF- $\beta$ 1 to induce EMT in renal tubular epithelial cells HK-2, and the results microscopic observations and functional experiments demonstrated the transformation of epithelial cells toward a mesenchymal state. Moreover, our results also verified that the promoting effects of TGF- $\beta$ 1 on the EMT and the proliferation and migration abilities of the renal tubular epithelial cells were achieved by inducing the phosphorylation of ERK and STAT3. In a previous study, overexpression of ERK could restrain renalase-mediated inhibition on TGF- $\beta$ 1-induced EMT and fibrosis, leading to the development of RIF (Wu et al. 2017).

ERK signaling pathway can be activated by a variety of stimuli, and plays profound and pervasive roles in development, physiology, and diseases (de la Cova et al. 2017). ERK acts as a pro-fibrotic factor important for inflammatory responses in renal fibrosis (Higgins et al. 2017). ERK has been shown to participate in EMT progression, and the inhibition of ERK contributes to ameliorating renal interstitial fibrosis by suppressing tubular EMT (Qin et al. 2015; Cheng et al. 2016). In addition to ERK, STAT3 was also studied as a downstream factor in our experiment, and the expressions

of p-ERK and p-STAT3 were remarkably increased in TGF- $\beta$ 1-induced renal tubular epithelial cells. In a previous report, complement C3 generated by macrophages promotes renal fibrogenesis through increasing pro-inflammatory cytokines and renal recruitment of inflammatory cells *via* mediating

the phosphorylation of ERK, STAT3, and STAT5 (Liu et al. 2018). Our results suggested that AFG was capable of inhibiting the activation of ERK/STAT3 signaling pathway, leading to reductions in EMT process, proliferation, and migration of TGF- $\beta$ 1-induced renal tubular epithelial cells.

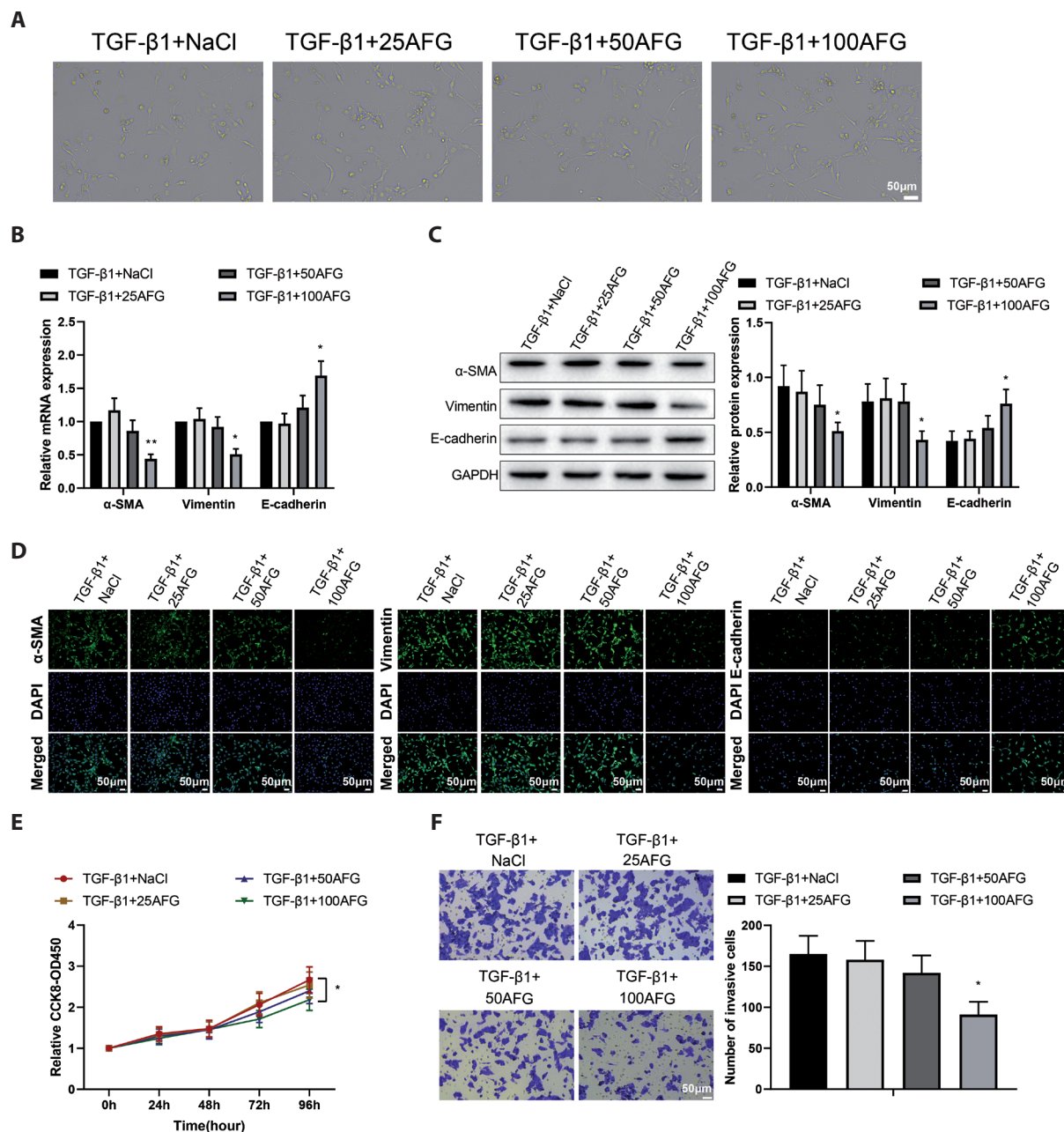


**Figure 4.** Arginyl-fructosyl-glucose inhibited TGF- $\beta$ 1-induced epithelial-mesenchymal transition in HK-2 cells. **A**, The morphology of HK-2 cells was observed under an inverted microscope. The expressions of  $\alpha$ -SMA, Vimentin, and E-cadherin were measured by qRT-PCR (**B**), Western blot (**C**), and immunofluorescence (**D**). Cell proliferation and invasion were evaluated by CCK-8 (**E**) and transwell (**F**) assays. \*  $p < 0.05$ , \*\*  $p < 0.01$  compared with TGF- $\beta$ 1+NaCl group. The measurement data were expressed as mean  $\pm$  SD ( $n = 15$  for immunofluorescence and transwell tests;  $n = 9$  for other experiments). Comparisons among multiple groups were performed using one-way analysis of variance or repeated analysis of variance. The scale = 50  $\mu$ m.

In cisplatin (CDDP)-induced acute kidney injury (AKI), AFG could inhibit oxidative stress, inflammatory response, and apoptosis, and had a protective effect on kidney (Li et al. 2019). Ginsenoside Rg1 (G-Rg1), isolated and purified from *Panax ginseng*, was reported to be beneficial for ameliorating renal fibrosis through suppressing the EMT process by targeting Klotho/TGF- $\beta$ 1/Smad signaling (Li et al. 2018). Ginsenoside Rb1 might restore cardiac and mitochondrial function and protect against cardiac remodeling *via* inhibiting the TGF- $\beta$ 1/Smad and ERK signaling pathways (Zheng et al. 2017). Ginsenoside Rh2 could also reduce the activation of STAT3 to function its anti-fibrotic effect in cardiomyocytes (Lo et al. 2017). Our findings confirmed, for the first time, that a non-saponin active substance AFG in red ginseng could restrain the EMT process, growth, and migration of renal tubular epithelial cells through inhibiting the activation of the ERK/STAT3 signaling pathway.

Collectively, these data showed that TGF- $\beta$ 1 could regulate ERK/STAT3 signaling pathway to promote EMT in renal tubular epithelial cells. In addition, we identified that ERK/STAT3 was an essential signaling pathway, thereby deepening our molecular understanding of how TGF- $\beta$ 1 induces EMT. Moreover, AFG has been proven to have the inhibiting effect on TGF- $\beta$ 1-induced EMT. To conclusion, our findings demonstrated that AFG played a significant role in TGF- $\beta$ 1-induced EMT development of renal tubular epithelial cells, modulated by the ERK/STAT3 signaling pathway. A new insight is brought by our findings, concerning the prevention and treatment of RIF.

**Acknowledgements.** We acknowledge Prof. Xiaoling Zou gave important advice to our article. We acknowledge Prof. Huzhi Cai provided the experimental space/reagent consumables free of charge, and thanks to all reviewers.

**Conflicts of interests.** The authors declare there is no conflict of interest regarding the publication of this paper.

**Funding.** This study was supported by the Scientific Research Project of Hunan Provincial Education Department (No. 18B240), Hunan University of Traditional Chinese Medicine Open Fund of First-class Discipline of Traditional Chinese Medicine (No. 2018ZYX28), Hunan University of Traditional Chinese Medicine School-level Research Fund Project (No. 2018XJJJ09).

## References

- Cheng X, Zheng X, Song Y, Qu L, Tang J, Meng L, Wang Y (2016): Apocynin attenuates renal fibrosis via inhibition of NOXs-ROS-ERK-myofibroblast accumulation in UUO rats. *Free Radic. Res.* **50**, 840-852  
<https://doi.org/10.1080/10715762.2016.1181757>
- de la Cova C, Townley R, Regot S, Greenwald I (2017): A real-time biosensor for ERK activity reveals signaling dynamics during *C. elegans* cell fate specification. *Dev. Cell* **42**, 542-553 e544  
<https://doi.org/10.1016/j.devcel.2017.07.014>
- Ghosh R, Siddarth M, Kare PK, Banerjee BD, Kalra OP, Tripathi AK (2021): beta-Endosulfan-mediated induction of pro-fibrotic markers in renal (HK-2) cells in vitro: A new insight in the pathogenesis of chronic kidney disease of unknown etiology. *Environ. Toxicol.* **36**, 2354-2360  
<https://doi.org/10.1002/tox.23349>
- Gupta N, Buffa JA, Roberts AB, Sangwan N, Skye SM, Li L, Ho KJ, Varga J, DiDonato JA, Tang WHW, Hazen SL (2020): Targeted inhibition of gut microbial trimethylamine N-oxide production reduces renal tubulointerstitial fibrosis and functional impairment in a murine model of chronic kidney disease. *Arterioscler. Thromb. Vasc. Biol.* **40**, 1239-1255  
<https://doi.org/10.1161/ATVBAHA.120.314139>
- Higgins DF, Ewart LM, Masterson E, Tennant S, Grebnev G, Prunotto M, Pomposiello S, Conde-Knape K, Martin FM, Godson C (2017): BMP7-induced-Pten inhibits Akt and prevents renal fibrosis. *Biochim. Biophys. Acta Mol. Basis Dis.* **1863**, 3095-3104  
<https://doi.org/10.1016/j.bbadis.2017.09.011>
- Higgins SP, Tang Y, Higgins CE, Mian B, Zhang W, Czekay RP, Samarakoon R, Conti DJ, Higgins PJ (2018): TGF-beta1/p53 signaling in renal fibrogenesis. *Cell Signal.* **43**, 1-10  
<https://doi.org/10.1016/j.cellsig.2017.11.005>
- Hsieh YH, Hung TW, Chen YS, Huang YN, Chiou HL, Lee CC, Tsai JP (2021): In vitro and in vivo antifibrotic effects of fraxetin on renal interstitial fibrosis via the ERK signaling pathway. *Toxins (Basel)* **13**, 474  
<https://doi.org/10.3390/toxins13070474>
- Hu J, Qiao J, Yu Q, Liu B, Zhen J, Liu Y, Ma Q, Li Y, Wang Q, Wang C, Lv Z (2021): Role of SIK1 in the transition of acute kidney injury into chronic kidney disease. *J. Transl. Med.* **19**, 69  
<https://doi.org/10.1186/s12967-021-02717-5>
- Jha V, Garcia-Garcia G, Iseki K, Li Z, Naicker S, Plattner B, Saran R, Wang AY, Yang CW (2013): Chronic kidney disease: global dimension and perspectives. *Lancet* **382**, 260-272  
[https://doi.org/10.1016/S0140-6736\(13\)60687-X](https://doi.org/10.1016/S0140-6736(13)60687-X)
- Ji T, Su SL, Zhu Y, Guo JM, Qian DW, Tang YP, Duan JA (2019): The mechanism of mulberry leaves against renal tubular interstitial fibrosis through ERK1/2 signaling pathway was predicted by network pharmacology and validated in human tubular epithelial cells. *Phytother. Res.* **33**, 2044-2055  
<https://doi.org/10.1002/ptr.6390>
- Kang DH (2018): Hyperuricemia and progression of chronic kidney disease: role of phenotype transition of renal tubular and endothelial cells. *Contrib. Nephrol.* **192**, 48-55  
<https://doi.org/10.1159/000484278>
- Karunasagara S, Hong GL, Park SR, Lee NH, Jung DY, Kim TW, Jung JY (2020): Korean red ginseng attenuates hyperglycemia-induced renal inflammation and fibrosis via accelerated autophagy and protects against diabetic kidney disease. *J. Ethnopharmacol.* **254**, 112693  
<https://doi.org/10.1016/j.jep.2020.112693>
- Lee JE, Park JJ, Myung CH, Hwang JS (2017): Inhibitory effects of ginsenosides on basic fibroblast growth factor-induced melanocyte proliferation. *J. Ginseng. Res.* **41**, 268-276

- <https://doi.org/10.1016/j.jgr.2016.05.001>
- Li RY, Zhang WZ, Yan XT, Hou JG, Wang Z, Ding CB, Liu WC, Zheng YN, Chen C, Li YR, Li W (2019): Arginyl-fructosyl-glucose, a major maillard reaction product of red ginseng, attenuates cisplatin-induced acute kidney injury by regulating nuclear factor kappaB and phosphatidylinositol 3-kinase/protein kinase B signaling pathways. *J. Agric. Food Chem.* **67**, 5754-5763  
<https://doi.org/10.1021/acs.jafc.9b00540>
- Li SS, He AL, Deng ZY, Liu QF (2018): Ginsenoside-Rg1 protects against renal fibrosis by regulating the Klotho/TGF-beta1/Smad signaling pathway in rats with obstructive nephropathy. *Biol. Pharm. Bull.* **41**, 585-591  
<https://doi.org/10.1248/bpb.b17-00934>
- Liu X, Liu W, Ding C, Zhao Y, Chen X, Khatoun S, Zheng Y, Cheng Z, Xi G (2020): Antidiabetic effects of arginyl-fructosyl-glucose, a nonsaponin fraction from ginseng processing in streptozotocin-induced type 2 diabetic mice through regulating the PI3K/AKT/GSK-3beta and Bcl-2/Bax signaling pathways. *Evid. Based Complement. Alternat. Med.* **2020**, 3707904  
<https://doi.org/10.1155/2020/3707904>
- Liu Y, Wang K, Liang X, Li Y, Zhang Y, Zhang C, Wei H, Luo R, Ge S, Xu G (2018): Complement C3 produced by macrophages promotes renal fibrosis via IL-17A secretion. *Front. Immunol.* **9**, 2385  
<https://doi.org/10.3389/fimmu.2018.02385>
- Lo SH, Hsu CT, Niu HS, Niu CS, Cheng JT, Chen ZC (2017): Ginsenoside Rh2 improves cardiac fibrosis via PPARdelta-STAT3 signaling in type 1-like diabetic rats. *Int. J. Mol. Sci.* **18**, 1364  
<https://doi.org/10.3390/ijms18071364>
- Ma J, Zhang L, Hao J, Li N, Tang J, Hao L (2018): Up-regulation of microRNA-93 inhibits TGF-beta1-induced EMT and renal fibrogenesis by down-regulation of Orai1. *J. Pharmacol. Sci.* **136**, 218-227  
<https://doi.org/10.1016/j.jphs.2017.12.010>
- Morikawa M, Derynck R, Miyazono K (2016): TGF-beta and the TGF-beta family: context-dependent roles in cell and tissue physiology. *Cold Spring Harb. Perspect. Biol.* **8**, a021873  
<https://doi.org/10.1101/cshperspect.a021873>
- Pan J, Shi M, Guo F, Ma L, Fu P (2021): Pharmacologic inhibiting STAT3 delays the progression of kidney fibrosis in hyperuricemia-induced chronic kidney disease. *Life Sci.* **285**, 119946  
<https://doi.org/10.1016/j.lfs.2021.119946>
- Park SM, Jung EH, Kim JK, Jegal KH, Park CA, Cho IJ, Kim SC (2017): 20S-Protopanaxadiol, an aglycosylated ginsenoside metabolite, induces hepatic stellate cell apoptosis through liver kinase B1-AMP-activated protein kinase activation. *J. Ginseng. Res.* **41**, 392-402  
<https://doi.org/10.1016/j.jgr.2017.01.012>
- Qin J, Mei WJ, Xie YY, Huang L, Yuan QJ, Hu GY, Tao LJ, Peng ZZ (2015): Fluorofenidone attenuates oxidative stress and renal fibrosis in obstructive nephropathy via blocking NOX2 (gp91phox) expression and inhibiting ERK/MAPK signaling pathway. *Kidney Blood Press Res.* **40**, 89-99  
<https://doi.org/10.1159/000368485>
- Wan Y, Wang J, Xu JF, Tang F, Chen L, Tan YZ, Rao CL, Ao H, Peng C (2021): Panax ginseng and its ginsenosides: potential candidates for the prevention and treatment of chemotherapy-induced side effects. *J. Ginseng. Res.* **45**, 617-630  
<https://doi.org/10.1016/j.jgr.2021.03.001>
- Wang F, Park JS, Ma Y, Ma H, Lee YJ, Lee GR, Yoo HS, Hong JT, Roh YS (2021): Ginseng saponin enriched in Rh1 and Rg2 ameliorates nonalcoholic fatty liver disease by inhibiting inflammation activation. *Nutrients* **13**, 856  
<https://doi.org/10.3390/nu13030856>
- Wang Y, Guo YF, Fu GP, Guan C, Zhang X, Yang DG, Shi YC (2020): Protective effect of miRNA-containing extracellular vesicles derived from mesenchymal stromal cells of old rats on renal function in chronic kidney disease. *Stem Cell Res. Ther.* **11**, 274  
<https://doi.org/10.1186/s13287-020-01792-7>
- Wu Y, Wang L, Deng D, Zhang Q, Liu W (2017): Renalase protects against renal fibrosis by inhibiting the activation of the ERK signaling pathways. *Int. J. Mol. Sci.* **18**, 855  
<https://doi.org/10.3390/ijms18050855>
- Yu J, Yu C, Feng B, Zhan X, Luo N, Yu X, Zhou Q (2019): Intrarenal microRNA signature related to the fibrosis process in chronic kidney disease: identification and functional validation of key miRNAs. *BMC Nephrol.* **20**, 336  
<https://doi.org/10.1186/s12882-019-1512-x>
- Zhang Y, Li H, Zhu J, Wei T, Peng Y, Li R, Xu R, Li M, Xia A (2017): Role of artesunate in TGFbeta1-induced renal tubular epithelial-mesenchymal transdifferentiation in NRK52E cells. *Mol. Med. Rep.* **16**, 8891-8899  
<https://doi.org/10.3892/mmr.2017.7728>
- Zheng X, Wang S, Zou X, Jing Y, Yang R, Li S, Wang F (2017): Ginsenoside Rb1 improves cardiac function and remodeling in heart failure. *Exp. Anim.* **66**, 217-228  
<https://doi.org/10.1538/expanim.16-0121>

Received: December 28, 2021

Final version accepted: May 20, 2022